



Employing Deep Learning Techniques for the Identification and Assessment of Skin Cancer

Sowmya Koneru¹, Pappula Madhavi², Krishna Kishore Thota³, Janjhyam V. Naga Ramesh⁴, Venkata Nagaraju Thatha⁵, S. Phani Praveen^{*6}

¹Department of CSE, Dhanekula Institute of Engineering & Technology, Vijayawada, A.P, India

²Department of Artificial Intelligence and Data Science, Lakireddy Bali Reddy College of Engineering, Mylavaram, A.P, India

³Department of CSE (Honors), Koneru Lakshmaiah Education Foundation (Deemed to be University), Vaddeswaram, A.P, India

⁴Adjunct Professor, Department of CSE, Graphic Era Hill University, Dehradun, India and Graphic Era Deemed to be University, Dehradun, 248002, India.

⁵Department of Information Technology, MLR Institute of Technology, Hyderabad, India

⁶Department of CSE, PVP Siddhartha Institute of Technology, Vijayawada, A.P, India

Emails: konerusowmya@gmail.com¹; pappulamadhavi06@gmail.com²; tkrishnakishore@kluniversity.in³; jvnramesh@gmail.com⁴; nagaraju.thatha@gmail.com⁵; phani.0713@gmail.com^{*6}

Abstract

These days, skin cancer is a prominent cause of death for people. Skin cancer is the name given to the abnormal development of skin cells that are exposed to the sun. These skin cells can develop anywhere on the human body. The majority of malignancies are treatable in the early stages. Thus, early detection of skin cancer is anticipated in order to preserve patient life. With cutting edge innovation, it is possible to detect skin cancer early on. Here, we provide a novel framework for the recognition of dermo duplication pictures that makes use of a neighbouring descriptor encoding method and deep learning technique. Specifically, the deep representations of a rescaled dermo duplication image that were initially removed through training an extraordinarily deep residual neural network on a big dataset of normal images. Subsequently, the neighbourhood deep descriptors are obtained by request-less visual measurement highlights, which rely on fisher vector encoding to create an international image representation. Lastly, a convolution neural network (CNN) was utilised to orchestrate melanoma images employing the Fisher vector encoded depictions. This proposed technique can give more discriminative parts to oversee huge contrasts inside melanoma classes and little varieties among melanoma and non-melanoma classes with least readiness information.

Keywords: Neural networks; skin cancer; deep learning methodologies; Machine-driven learning; Identification; Assessment.

1. Introduction

It is possible for cancer to spread to distant parts of the body since it is caused by the uncontrolled division of neurotic cells. It is possible for the skin to play a vital role in the human body by providing protection to the bones and muscles in every other region of the body. Assuming that the functionalities of the skin wander somewhat, the entire body structure becomes disrupted, which has an effect on all of the essential capacities of the body. The most prevalent and dangerous form of cancer is skin cancer, which is also the most common type of cancer overall. When it is discovered in its early stages, skin cancer has the potential to be treated and perhaps surgically removed. The hurting region is sometimes referred to as the skin mark that has been wiped out. There is a wide variety of skin injuries that can be experienced. Any kind of injury is separated from the structure of the skin cells that causes the commencement of the harm. Melanocytes, known as melanoma, are responsible for the development of melanocytic lesions, which are essential for the production of a protein pigment known as melanin. Certain cell structures of the skin, such as basal or squamous cells, are responsible for injuries that are not to the melanocytic cells. There are two separate categories of injuries, which are differentiated from one another based on the availability of a succession of dermoscopic components, such as a shade organisation, or the absence of such components [1].

It is estimated that twelve million individuals are afflicted with cancer, with skin cancer being the primary concern for western nations, particularly the United States of America, which has a continuous daylight exposure. In the United States of America in the year 2020, there will be around one million new cases of skin cancer. When attempting to differentiate between malignant cells and skin cancer, the most fundamental method of diagnosis is to examine the skin from the outside by a dermatologist who specialises in the field. It is difficult to provide specialised dermatologists and therapeutic assistance to each and every individual, and the majority of the time, people do not seek the assistance of specialists until the condition has progressed to the point where they want to be treated [2].

The biopsy approach is typically differentiated by medical professionals when it comes to diagnosing infections. In the course of the biopsy cycle, the skin is either rejected or withdrawn, and the particular research facility inspections that are conducted on these skin tests can be carried out. Along these lines, this engagement is time-consuming and frequently unclear. It is also time-consuming. Beginning phase diagnosis of skin cancer is made possible by the use of PC-supported screening. The majority of the time, plainly visible photographs are categorised as quantifiable photographs that are utilised for the most part for the management of personal computers. These photographs are captured with a standard computer camera and video. Clinical photographs contain a number of drawbacks, such as inadequate lighting and the existence of peculiarities, such as skin lines, features, redundancy, and hair in the photographs. As a direct consequence of these challenges, conducting an investigation into skin injuries is an incredibly tough task. At the computational level, there are a few steps that are involved in differentiating skin cancer. These steps include pre-processing, recognising patterns, selecting elements, and extracting highlights and identification [3].

To eliminate symbolism, the initial step involves removing specific elements. When categorizing lesions, attributes are the logical focus.

There is the possibility of removing properties, which may then be separated into global and local capability extraction methods. Neural networks have the potential to perform similarly as capability extractors. Following this, the exceptional components will be separated, and the resulting document will be in accordance with the type of document. The determination of capabilities that are appropriate results in a high level of accuracy and security, and it also allows the classifier to convey its findings. The use of PC vision allows for a wide variety of inferences to be made regarding the components of dermoscopic and non-dermoscopic objects. Recently, there have been a few attempts made in the field of healthcare innovation to investigate deep learning strategies for the purpose of image classification and division. A CNN model was utilised by the authors in order to work with skin cancer detection. Additionally, a multitude of skin lesions photographs were utilised in order to categorise them as either cancerous or non-cancerous. In order to provide assistance to medical professionals in identifying patients with high needs, the designers merged the CNN model into a web-based platform. [4].

This paper offers an overview of the related work in section 2, background in section 3 used material and methods in section 4, section 5 provides the results and discussion of the experimental research and finally, section 6 provides the conclusions and future work of this paper.

1.1. Contributions

- a. Researchers contribute by developing novel deep learning architectures tailored for skin cancer detection, enhancing accuracy.
- b. Writers disseminate knowledge through academic papers, articles, and reports, fostering awareness and understanding of deep learning's role in skin cancer diagnosis.
- c. They contribute to the refinement of deep learning models by critiquing methodologies, suggesting improvements, and promoting collaboration within the research community.
- d. Writers play a pivotal role in translating complex technical concepts into accessible language, bridging the gap between deep learning research and clinical practice in skin cancer diagnosis.

2. Review Of Literature

Mazhar et.al [5] gives a thorough assessment of the job that deep learning and machine learning play in the recognizable proof of skin cancer. The focus likely delves into a variety of ML and DL computations, evaluating their feasibility in analysing photos of skin sores for didactic reasons. Through an examination of the intricate details and performance metrics of these computations, the authors hope to make a significant contribution to the field of simulated intelligence-driven solutions that will improve the accuracy and efficiency of skin cancer diagnosis. The review might discuss the challenges and important opportunities associated with these methods and make recommendations for potential directions for further research.

Gouda et.al [6] specifically highlight the application of deep learning for skin cancer identification in light of photos of skin sores in their June 2022 distribution. The focus most likely on the abilities of deep learning models—like neural networks—to learn complex examples and highlights from enormous databases.

The authors may discuss the specific deep learning architecture that was used, its training process, and the achieved results in terms of responsiveness, explicitness, and overall accuracy.

Hossin et.al [7] combines state-of-the-art regularizer processes with deep learning to develop an innovative methodology with melanoma skin cancer identification. The examination, which was introduced at the Global Gathering on Cutting edge Programming and Information Structures, may take a gander at the specific complexities of the deep learning model that is being utilized. It also emphasises the role that advanced regularizers have in improving the model's prediction and implementation. The review could showcase trial findings that demonstrate the feasibility of the suggested approach in accurately differentiating between melanoma and skin cancer. By specifically focusing on the location of melanoma, this work contributes to the growing field of deep learning applications in clinical picture examination.

Viriri and Adegun et.al [8] concentrate, which was released in the Man-made Consciousness Survey in 2021, adopts a more comprehensive stance by presenting a research of state-of-the-art deep learning techniques for melanoma cancer detection and skin sore assessment. The authors likely lead a thorough overview of the literature already in existence, summarising significant developments, frameworks, and challenges in the field. This research may address various deep learning architectures, data sources, and performance metrics applied to melanoma detection. Adegun and Viriri provide a thorough overview of the current state of deep learning applications in melanoma location by coordinating the findings from numerous studies, providing crucial information for researchers and experts in the field.

Bassel et al. [9] focuses on enhancing a structured skin cancer classification system by the utilisation of a hybrid deep learning methodology. The analysis most likely delves into the nuances of the mixed model, which may combine various deep learning architectures or synchronise deep learning with traditional machine learning techniques. The evaluation should highlight the model's performance in differentiating between dangerous and benign skin lesions by introducing important metrics including responsiveness, particularity, and overall precision. The study conducted by Bassel et al. adds to the increasing amount of research that delves into new ways of improving skin cancer detection accuracy through the integration of several computer methodologies.

Tembhurne et al. [10] offer an optional method for dealing with the diagnosis of skin cancer in their 2023 publication in *Mixed media Apparatuses and Applications*. The focus is likely on the cooperative energies between models within the group, examining how combining the features of diverse calculations improves overall demonstration precision. The decision-making processes for models within the group, the preparatory dialogue, and the ensuing implementation of the plan might all be discussed by the authors. Research highlights the potential benefits of combining both conventional machine learning and deep learning as one for improved skin cancer identification, contributing to the expanding body of hybrid approaches.

Adla et al. [11] focus is on presenting a PC-supported decision model with deep learning that is specifically designed for skin cancer identification and characterization. The investigation most likely delves into the design and architecture of the deep learning model, defining the specific neural network architectures, setting up procedures, and taking execution metrics into account.

The authors may also discuss the dataset that was used for preparation and approval, as well as the final results in terms of awareness, explicitness, and overall accuracy. The work of Adla et al. extends our understanding of the potential logical use of deep learning to dermatological diagnoses by providing tidbits of information on the capabilities of computer-aided design models for skin cancer.

Mixed media Devices and Applications published a paper by Nancy et al.[12] in 2023 that analyses skin cancer detection using deep learning and machine learning. The focus most likely evaluates how various computations are presented, considering aspects such as accuracy, computational ability, and conjecture over various datasets. By doing a comparable investigation, the authors hope to highlight the advantages and disadvantages of different approaches to the localization of skin cancer. The study by Nancy et al. contributes to a broader understanding of the viability of deep learning and conventional machine learning techniques for dermatological diagnosis.

Inthiyaz et al. [13] uses deep learning to uncover skin illnesses. The investigation most likely looks into applying deep learning models to a wider range of skin infections, providing a comprehensive approach to dermatological diagnoses. The authors may delve into the specific deep learning architectures employed, the preparation dataset, and the evaluation metrics employed to gauge the model's performance. By presenting new developments in the field, Inthiyaz et al. expand on our knowledge of the suitability and effectiveness of deep learning for diagnosing conditions other than skin cancer.

Ashraf et al. [14] presented at the 23rd IEEE Worldwide Multitopic Gathering in November 2020, this review offers a deep learning-based effective approach for skin cancer classification. The investigation likely reveals details about the specific deep learning model used, the preprocessing procedures used on images of skin injuries, and the overall framework for classifying skin cancers. The inventors may use metrics such as explicitness, awareness, and exactness to showcase how their approach is presented. The work of Ashraf et al. expands the specific body of knowledge about the identification of skin cancer, highlighting the need for effective and accurate grouping techniques to enhance early diagnosis and treatment.

3. Background

3.1. Convolutional Neural Network for Categorization of Images

The convolutional neural networks (CNN) that make up fake neural networks are given life by the real neurons that exist in our minds [15]. Because CNNs understand interpretation invariance, they are able to interpret a certain article in any event, no matter how it appears. This is a key feature that distinguishes CNN from feed-forward neural networks, which are unable to recognise interpretation invariance [16].

Stated differently, feed-forward neural networks exhibit recognition capabilities only for objects that are squarely in the centre of the image; when an object is positioned elsewhere or is slightly out of place, they manifestly fail to recognise it [17]. To put it simply, the network picks up knowledge from a single instance. Considering that the real datasets that are now available are frequently raw and organic, this is definitely not helpful [18].

3.2. Convolution Neural Networks' Operation

This begs the question, "How does CNN interpret interpretation invariance?" Could it be that machine learning works like magic? It all comes down to science once more [19]. The many CNN layers and phases are the corresponding duties.

3.2.1. Convolution

The primary operation, convolution, cleanses the image of irrelevant details. Since it's a numerical exercise, two information sources are definitely needed: a picture lattice and a channel or bit [20]. To include the map, the channel is increased with the pixel values and traversed through the image.

Figure 1 illustrates the process of the convolution procedure.

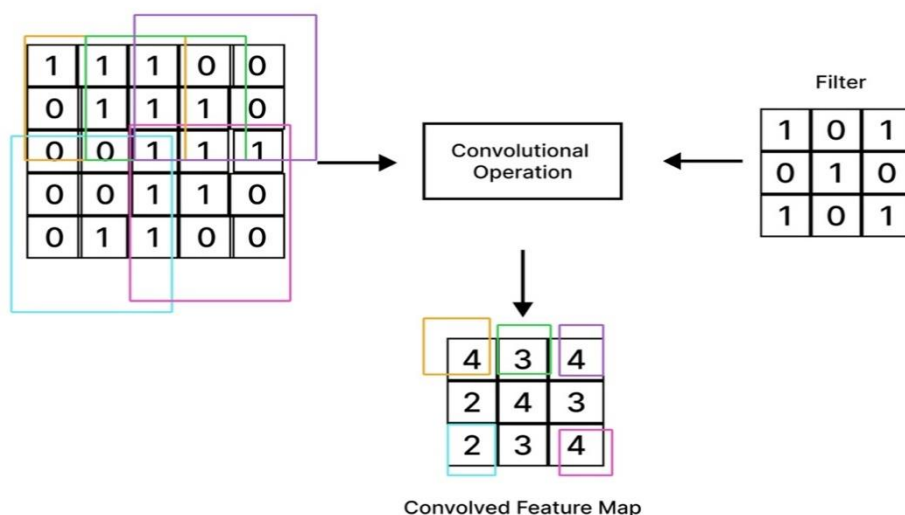


Figure 1: Convolutional process

Convolution results in data loss, but it also presents a chance to master the foundations and minimise size [21]. Picture processing activities like edge location, hiding, and picture sharpening can be aided by convolution using multiple types of channels.

3.2.2. Pooling

With very large images, pooling operations help to reduce the number of borders. Subsampling—also referred to as spatial pooling—reduces each element map's dimensionality while preserving massive amounts of data [22]. Pooling is a fundamental operation in neural networks, and it comes in three distinct forms. The most commonly used is Max Pooling, where the maximum value within a region is selected. Additionally, there is Sum Pooling, where the values within a region are summed, and Average Pooling, where the average value is calculated. These pooling techniques play a crucial role in reducing the spatial dimensions of the input data, aiding in feature extraction and dimensionality reduction in neural network architectures. Max pooling is one discretization technique that is example-based. In essence, the component map is updated with the quantity of values for each normal and aggregate pooling. Figure 2 shows how to use Max Pooling.

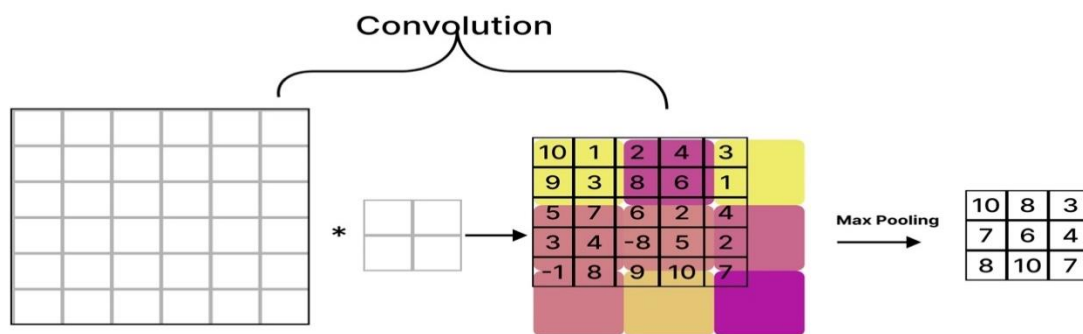


Figure 2: Max pooling Method

3.2.3. Flattening

We really require a single segment vector of the image pixels in order to handle our component mappings in the fake neural network [23]. We smooth our component maps into segment like vectors, as the name suggests. Figure 3 illustrates the act of flattening.



Figure 3: Flattening process

3.2.4. Full Connection

The completely associated layer accepts its contribution from the convolution/pooling layer before it, which creates a N-layered vector that demonstrates the quantity of classes that should be ordered [24]. Subsequently, the layer decides the qualities generally firmly connected to a specific class utilizing the neuronal probabilities. In figure 4 the completely linked layer of a neural network is displayed.

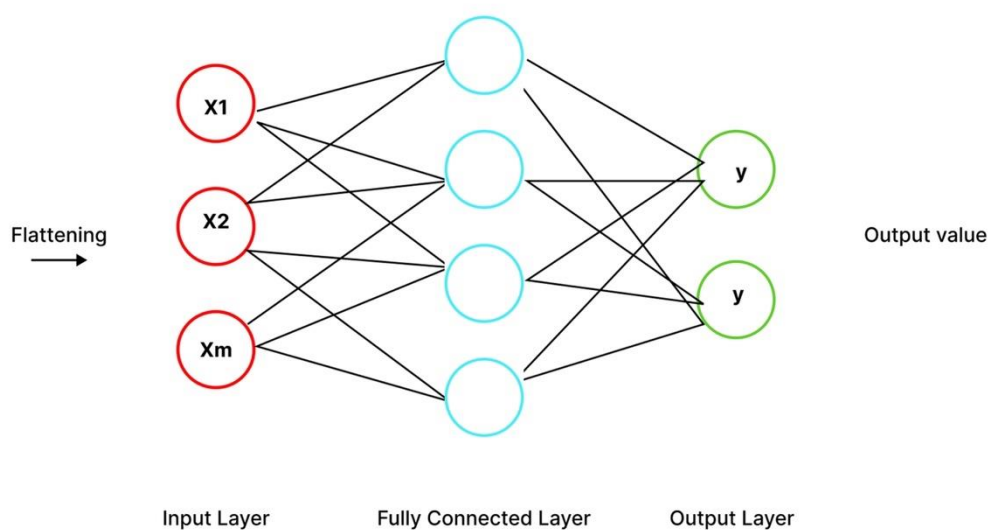


Figure 4: Whole layer of connection

3.3. CNN-Based Skin Lesion Classification

Prior studies in this field demonstrate CNN's distinct qualification to cure skin lesions in the face of expert dermatologist rivalry. On other occasions, CNN has even outperformed experienced dermatologists [25]. Skin sores can be classified by CNN using two different techniques. In the first example, the picture's elements are extracted using a CNN, and the images are then grouped by another classifier. Alternatively, start-to-finish learning—which is further separated into learning from a pretrained model and learning without any prior preparation—is executed using CNN [26].

To mitigate the overfitting problem, a large number of photos are expected to be ready for CNN. There aren't enough pictures of skin lesions to conduct the preparation, therefore it is less feasible to prepare CNN without any. This better strategy for preparing from a pretrained model is called Move Learning (TL) [27]. Moreover, TL assists the model with learning great even with little contribution by familiarizing the hypothesis property with the pre-arranged model [28].

4. Materials and Method

4.1. Dataset

The Global Skin Imaging Joint effort (ISIC): Melanoma Venture is an alliance of industry and academia that uses computerised skin imaging to try and lower the death rate from skin cancer. In 2022, ISIC initiated the worldwide skin sore investigation challenges aimed at identifying and localising melanoma. Figure 5 exhibits instances from the dataset representing each class.

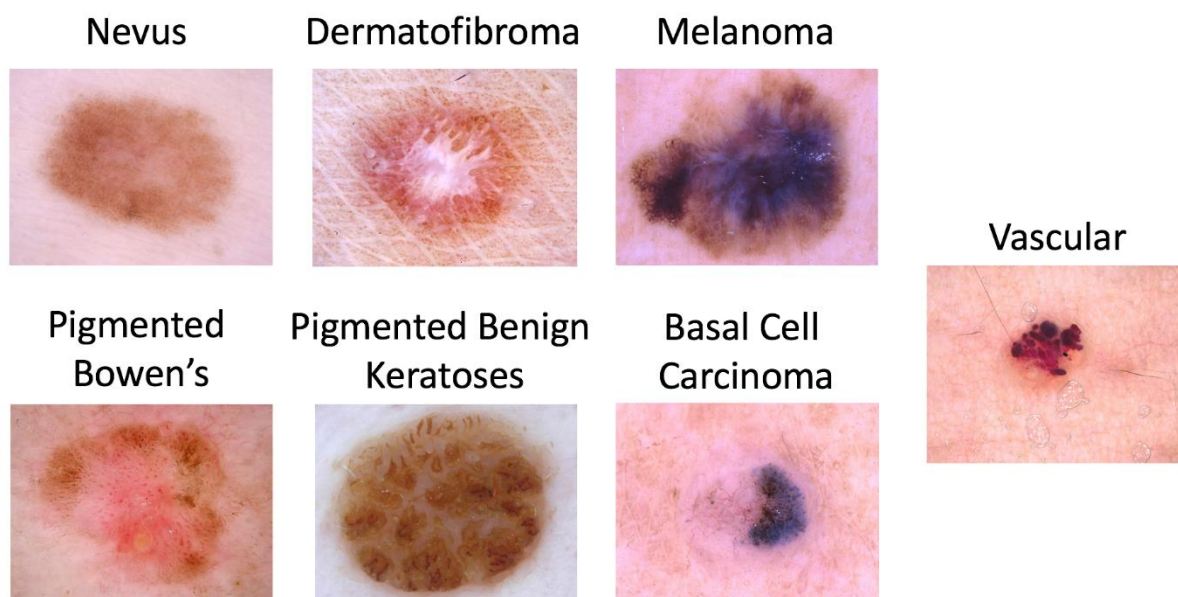


Figure 5: Various Skin Lesions in Increasing Order: An All-Inclusive ISIC Dataset Assembling

This project is supported by two datasets that were made available through a test that ISIC conducted in 2022 and 2023.

The first dataset, called "ISIC 2022," contains 10,016 pictures of seven different skin harm conditions. The Clinical School of Vienna and the School of Queensland endorsed the image assortment. Table 1 enumerates the first dataset utilized in this research.

Table 1: Data from the dataset ISIC 2022

Dataset	Type	Number of images	Image type	Class labels						
				0: Melanoma	1: Melanocytic Nevus	2: Basal Cell Carcinoma	3: Actinic Keratosis	4: Benign Keratosis	5: Dermatofibroma	6: Vascular Lesion
ISIC challenge 2022	Dermoscopic	10,016	JPEG (RGB)	0: Melanoma	1: Melanocytic Nevus	2: Basal Cell Carcinoma	3: Actinic Keratosis	4: Benign Keratosis	5: Dermatofibroma	6: Vascular Lesion

The second dataset, called "ISIC 2023," has 26,335 pictures of eight various types of skin injury diseases. Table 2 describes the dataset 2 that was utilised in this work.

Table 2: Details about the ISIC 2023 dataset

Data set	Type	Number of images	Image type	Class labels							
				0: Melanoma	1: Melanocytic Nevus	2: Basal Cell Carcinoma	3: Actinic Keratosis	4: Benign Keratosis	5: Dermatofibroma	6: Vascular Lesion	7: Squamous Cell Carcinoma
ISIC challenge 2023	Dermoscopic	26,335	JPEG (RGB)	0: Melanoma	1: Melanocytic Nevus	2: Basal Cell Carcinoma	3: Actinic Keratosis	4: Benign Keratosis	5: Dermatofibroma	6: Vascular Lesion	7: Squamous Cell Carcinoma

The datasets of ISIC 2022 and ISIC 2023 were combined to create a new dataset. Further noise was removed from the dataset, and the seven typical kinds of skin injuries were retained. The models were able to learn even more effectively given that there were so many tests available for every class. The final dataset utilised for this experiment is summarised in Table 3.

Table 3: Details about the final dataset

Data set	Type	Number of images	Image type	Class labels							
				0: Melanoma	1: Melanocytic Nevus	2: Basal Cell Carcinoma	3: Actinic Keratosis	4: Benign Keratosis	5: Dermatofibroma	6: Vascular Lesion	ISIC challenge 2022
ISIC challenge 2022	Dermoscopic	36,345	JPEG (RGB)	0: Melanoma	1: Melanocytic Nevus	2: Basal Cell Carcinoma	3: Actinic Keratosis	4: Benign Keratosis	5: Dermatofibroma	6: Vascular Lesion	ISIC challenge 2022

The number of photos supplied into the network by class is displayed in Table 4.

Table 4: Count of photos for each type of lesion

Lesion type	Quantity of pictures
0: Melanoma	5535
1: Melanocytic Nevus	20680
2: Basal Cell Carcinoma	3738
3: Actinic Keratosis	1292
4: Benign Keratosis	3623
5: Dermatofibroma	350
6: Vascular Lesion	400

4.2. Implementation Environment

The project utilized two datasets, namely ISIC 2022 and ISIC 2023, to construct a consolidated dataset comprising 36,345 dermoscopic images featuring seven distinct types of skin lesions, including melanoma, melanocytic nevus, basal cell carcinoma, actinic keratosis, benign keratosis, dermatofibroma, and vascular lesions. The images were formatted in JPEG (RGB), and data augmentation techniques such as editing, cushioning, noise addition, brightness adjustment, and level flipping were applied to enhance the diversity and volume of training data. Normalization was performed to ensure consistent pixel intensity gains, contributing to improved neural network performance.

Transfer learning with pre-trained weights from ImageNet was employed to enhance the training efficiency of CNN models, including MobileNet, Inception-Resnet, VGG16, ResNet50, and Inception V3. The implementation specified optimizer, learning rate, epochs, dropout rate, and other hyperparameters for training the CNN models. Model performance was evaluated using various criteria like accuracy, precision, recall, F1 score, and support, and the results were compared. Notably, the Inception V3 and Inception Resnet models exhibited the highest precision in skin lesion classification, achieving 94% and 95%, respectively. The implementation environment and outcomes of the skin lesion classification project were comprehensively detailed, presenting average metrics and learning curves for each model.

4.3. Database Discussed

The two primary datasets in the dataset, "ISIC 2022" and "ISIC 2023," provide a thorough analysis of the data. When examining the quantity of photos by type of lesion, the first part finds that "ISIC 2022" has 10,016 photos, whereas "ISIC 2023" has 26,335 photos. The many lesion categories include Actinic Keratosis, Benign Keratosis, Dermatofibroma, Melanoma, Melanocytic Nevus, Basal Cell Carcinoma, and Vascular Lesion. The number of photos for each category is explained in both datasets. The subsequent section provides a description of the image processing augmentation techniques employed, covering aspects such as Zoom, Rotation, Horizontal flip, Rescale, Width shift, and Height shift. Following that, the discussion transitions to the parameters utilized in model training, specifying information about the optimizer (Adam optimizer), batch size (65), dropout (0.5), learning rate (0.0002), epochs (35), and the loss function (categorical cross-entropy).

Confusion matrices and performance measures, including accuracy, recall, F1 score, and support for each dataset and model version (ResNet50, MobileNet, VGG16, Inception V3, InceptionResnet), are shown in the next section. These metrics provide a detailed insight of the models' effectiveness on both datasets and are thoroughly computed for different sorts of lesions. The last section summarises the overall performance of the models by combining the metrics for accuracy, precision, recall, F1 score, and support for each model for both datasets. In summary, the thorough discussion presents a thorough assessment of the model's performance via a variety of lenses, highlighting the subtleties of the datasets and offering insightful information for more research and development. The Overview of the classification model is in figure6.

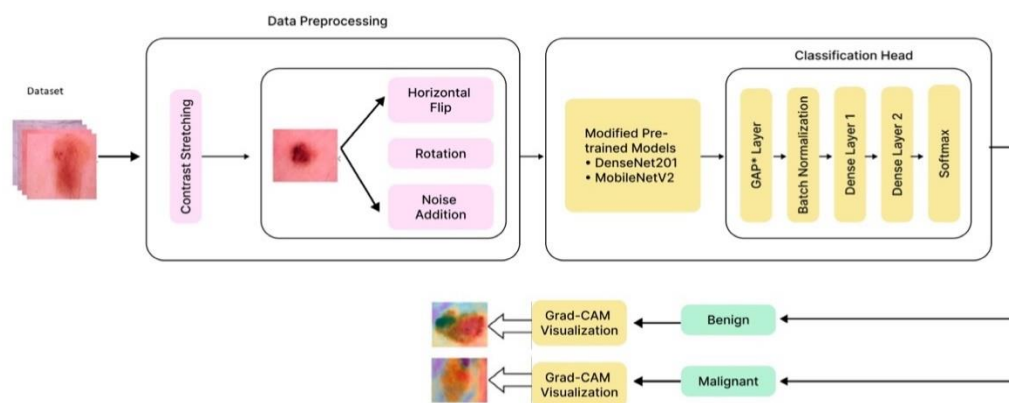


Figure 6: Overview of the classification model

4.3.1. Data Augmentation

Recent developments in deep learning models have typically been linked to vast amounts of diverse data. Massive amounts of information are really helpful when working on machine learning model presentations. Nevertheless, obtaining this vast amount of data is expensive and depressing [29]. As a result, we employ the information expansion strategy. With the use of a plan, we can greatly expand the range and quantity of information that is available without actually gathering new data [30]. Huge neural networks are typically prepared using a variety of techniques, such as editing, cushioning, adding noise, altering the splendour, and level flipping, in order to generate new information from an increasing number of photographs [31].

In order to improve testing accuracy, the training images in this study are improved to increase the model's resistance to new input [32]. The techniques for augmentation applied to the dataset are shown in Table 5.

Table 5: Details regarding the settings used for data augmentation

TECHNIQUE OF AUGMENTATION	RANGE
ZOOM RANGE	0.2
ROTATION RANGE	11
HORIZONTAL FLIP	False
RESCALE	1./256
WIDTH SHIFT RANGE	0.2
Height shift range	0.2

4.3.2. Normalisation of Images

To make the image's pixel potential gains uniform in a comparable medium, a cycle known as picture normalization is utilized. It is helpful to normalize pictures preceding taking care of them into the brain network since this expands the effectiveness of the slant plunge process by putting the worldwide minima at the blunder surface nearer together [33]. In a sense, it facilitates faster network integration. Furthermore, since the entire pixel values are scaled, the computations required for the machine to function become much less complex [34].

4.3.3. Transfer Learning

In a collaborative effort called move learning, a model developed for one task is used as a foundation for another model for a related task. This approach is popular in significant learning since cerebrum network model preparation consumes a huge piece of the day and a lot of taking care of resources [35]. Projects using data streams may have their low-level components—such as forms, corners, edges, and power—divided due to problems with the PC visual space. Move learning is utilized in this undertaking to make the CNN in light of the pretrained weight of ImageNet characterisation [36].

The characterisation task, known as the ImageNet Huge Scope Visual Acknowledgment Challenge (ILSVRC), comprises 18 million preparatory images representing almost 20,000 classes [37]. The classifier planning time is expanded, the impediment of restricted arrangement information is survived, and the opportunity of effective gathering is expanded when changes are made solely founded on the pretrained weight [38]. The pretrained weight makes it plausible for the pre-arranged model to change at a speedier speed, and the CNN's front layers effectively see the picture's corners, edges, and fundamental models [39]. The model is gathered and examined to determine the level of craftsmanship. CNNs will broadcast the photographs of the sore skin as a seven-class social event.

4.3.4. Dropout

Poor preparation tests on a dataset might lead to overfitting of Deep Neural Networks (DNNs). Although it is well-known that combining neural networks with diverse topologies can decrease overfitting, doing so requires us to create and maintain a variety of models, which can be computationally demanding [40]. Dropout enters the picture at this point. During preparation, a single model is used to appear to have many distinct network architectures by randomly leaving hubs. This is how dropout functions, and assuming nothing else changes, it indicates a computationally feasible and very convincing way to improve speculative mistakes and lessen overfitting in DNNs.

4.4. Network Architecture

4.4.1. Inception V3

Origin V3, a well-known image recognition model, was created over time by a number of specialists.

Drawing from Szegedy's original work "Reevaluating the Beginning Engineering for PC Vision," the model has demonstrated over 79% accuracy on the ImageNet dataset. The Beginning V3 network's model design is displayed in Figure 7. Google's proposed V3 Deep Learning Convolutional Model is the third cycle in the series. It is made up of beginning modules that apply channels of various sizes to comparable levels of data. The bottleneck layer, a more modest middle block, receives a shorter contribution due to the application of 1 x 1 convolution, which addresses the high calculation cost associated with the initiation module [41]. For regularisation purposes, the Commencement network's assistance classifiers increase the weighted misfortune capability.

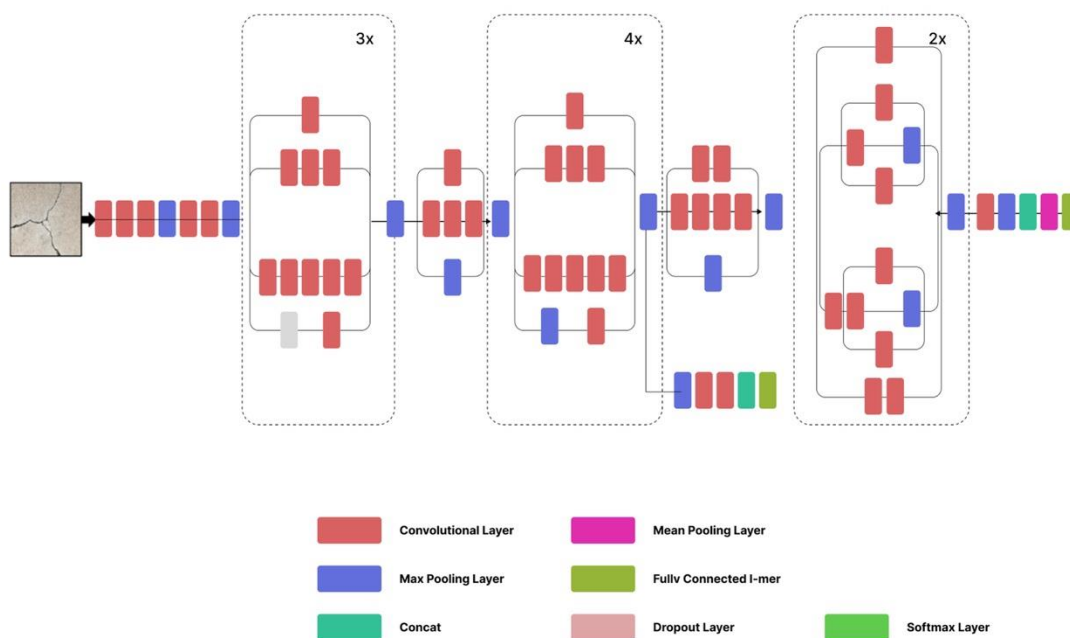


Figure 7: Inception V3 architecture

Factorization was a crucial addition to the Initiation V3. To decrease the overfitting issue, factorization was incorporated into the convolution layer to additionally diminish the dimensionality.

4.4.2. ResNet50

A number of PC vision projects rely on the widely used neural network model known as Residual Network (ResNet). This ResNet model triumphed in the 2015 ImageNet challenge [42]. A deep CNN typically has a large number of prepared and layered layers. Many low level, centre, and substantial level highlights are learned by the network. Instead of learning certain components, residual learning familiarises us with some that are still present.

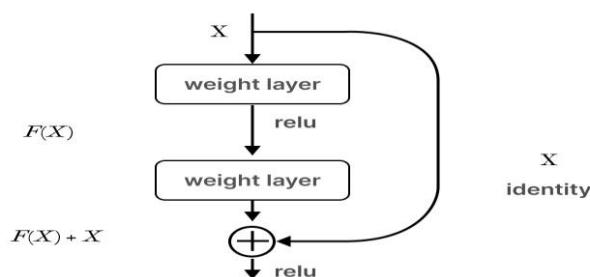


Figure 8: ResNet 50 model's residual block

4.4.3. VGG 16

The CNN model known as VGG16 was advanced by Oxford School specialists A. Zisserman and K. Simonyan in their distribution "Very Deep Convolutional Networks for Huge Scope Picture Affirmation." [43]. Figure 9 depicts the configuration of the VGG 16 network's model architecture.

A 225 x 225 RGB image is what this model must contribute. A multitude of convolutional layers are applied to the image, with a 4 x 4 component size or channel size. The step is set to one pixel, and the convolution layer input cushioning is set so that the spatial target is protected after convolution (for instance, for three-by-three convolution layers, the cushioning is one pixel). Max-pooling has been completed.

Three Fully Associated (FC) layers come after the pile of convolutional layers. There are 4095 channels in each of the two underlying levels, and 1100 channels in the third layer. The softmax enactment capability is included in the final layer. Any that are still tucked away have the non-linearity amendment (ReLU) enacted.

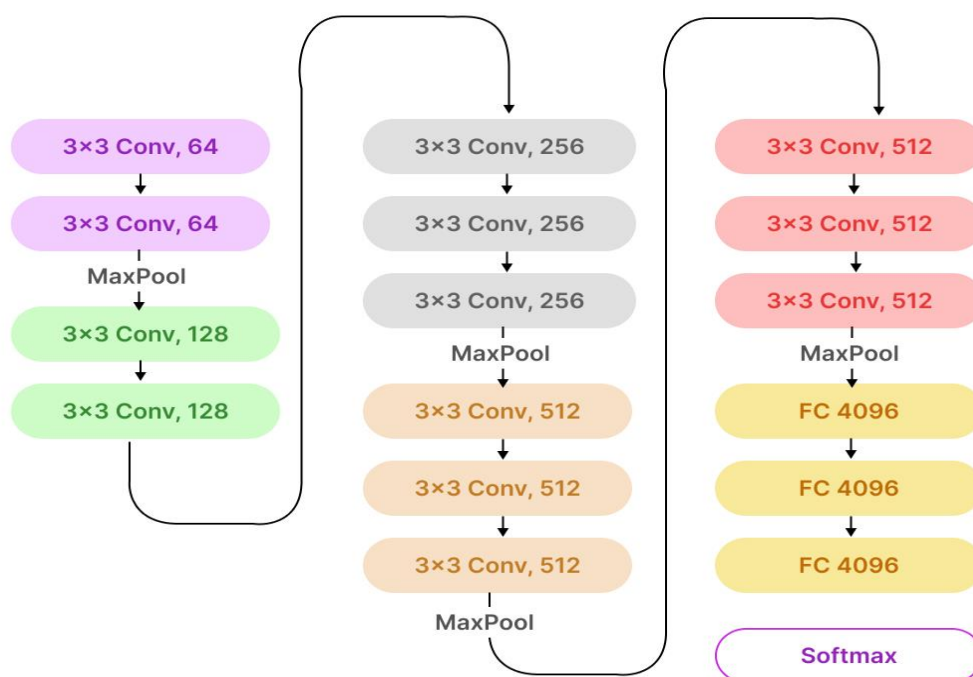


Figure 9: VGG 16 architecture

4.4.4. Inception-Resnet

Starting off A CNN model called ResNet-v2 was created using the ImageNet data set. With its 165 layers, it can classify images into 1100 categories. The network is dynamic and has acquired excellent element portrayals for a variety of films. A photograph with a resolution of 300 by 300 pixels must be contributed to the network. Generally speaking, Origin Resnet V2 is more affordable to create and calculate than Initiation V4. Additionally, it familiarises the remaining association with the submodules Origin Block A, B, and C on the passed on side so that the network can delve further [44]. The model design of the Commencement Resnet network is shown in Figure 10.

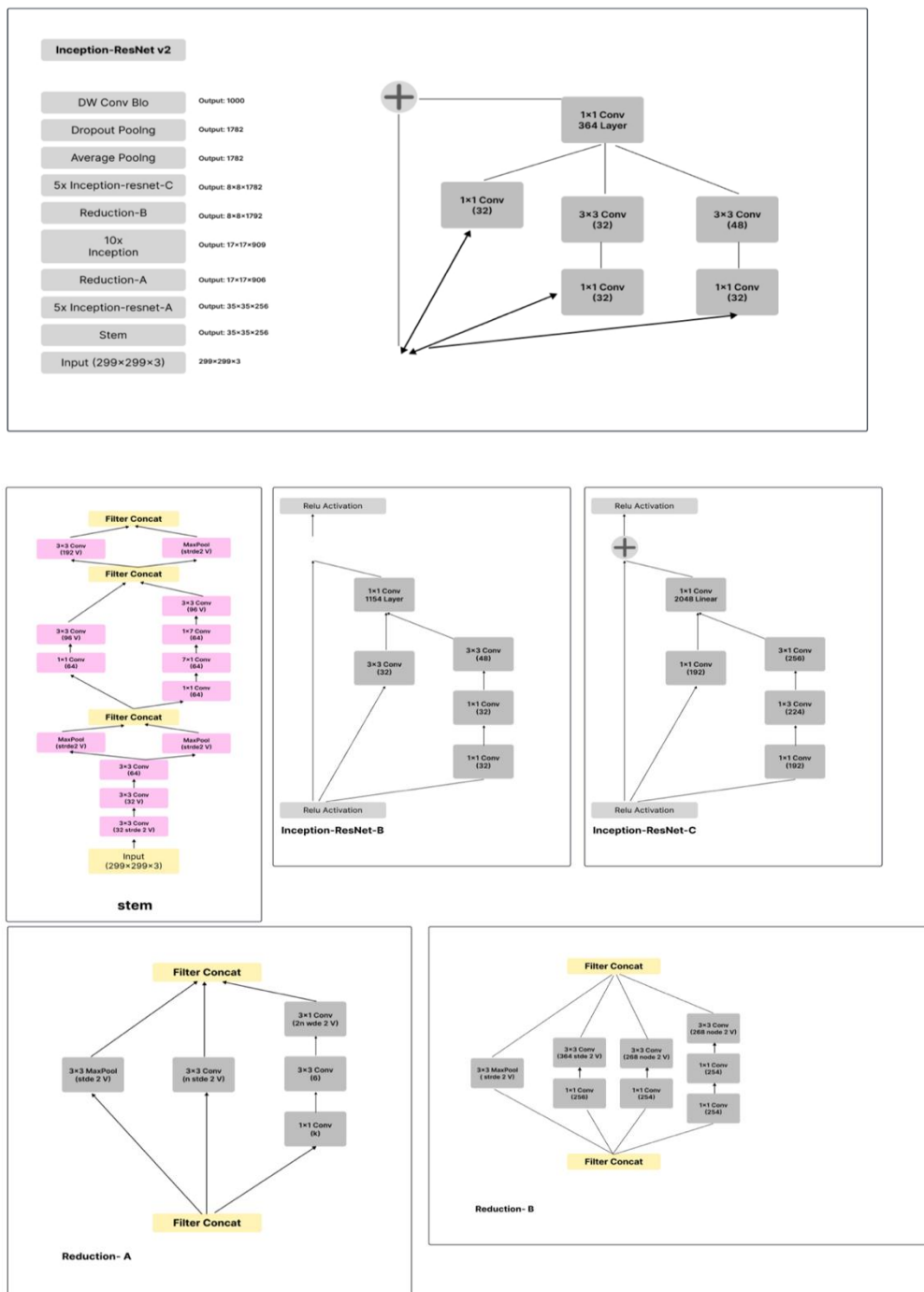


Figure 10: InceptionResnet architecture

Assist with making lightweight deep neural networks by bringing down the amount of learnable lines. Adaptive and newly-introduced PC vision applications benefit from its ability to reduce the total number of floating-point gauges needed for power management [45]. Figure 11 illustrates the convolution processes at both the point-wise and depth-wise levels. Figure 12 provides an overview of the design of the MobileNet CNN model.

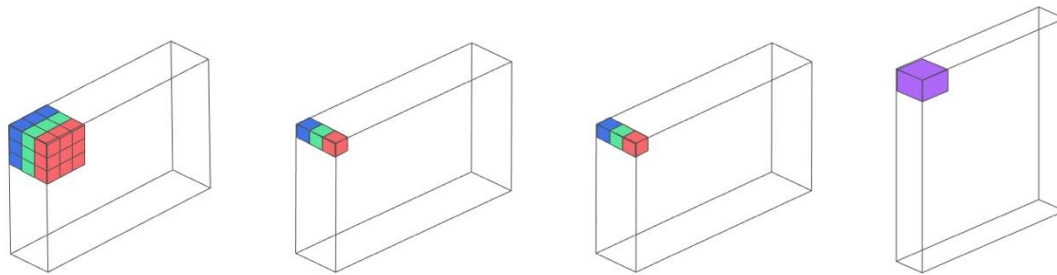


Figure 11: Convolution both point wise and depth wise

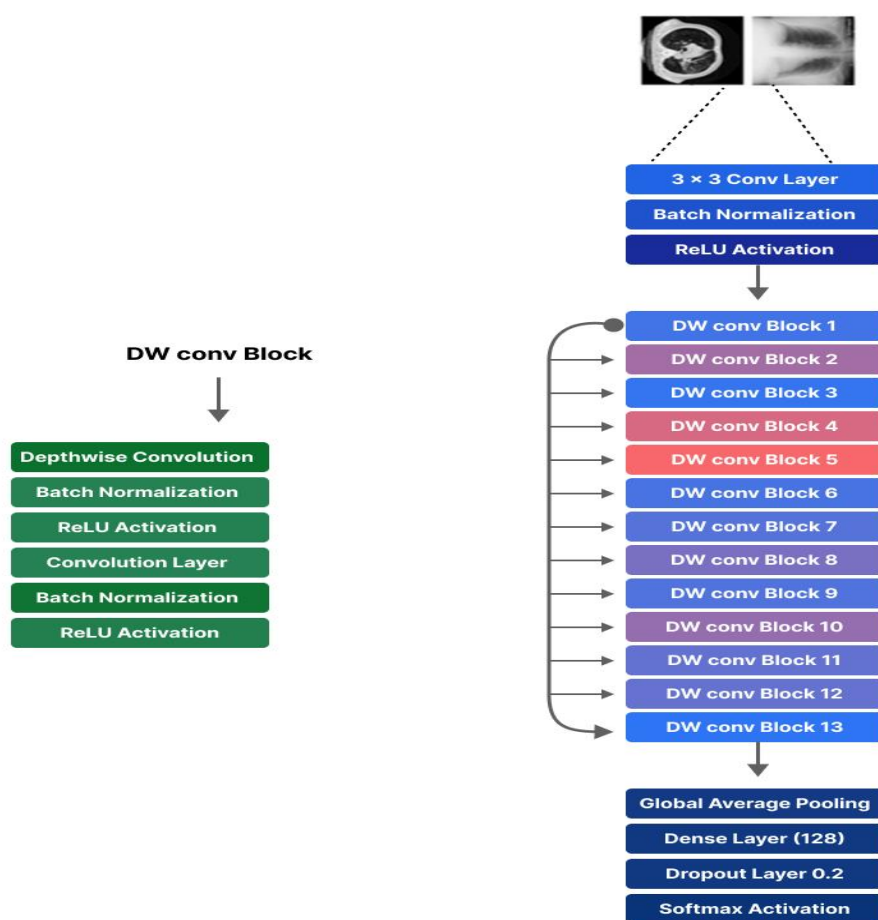


Figure 12: The MobileNet architecture

5. Experimental Results

5.1. Performance metrics

For example, a true positive scenario happens when the model predicts that the lesion is melanoma and the skin lesion image is tagged with melanoma. A false negative is when a photo is reported as having melanoma when, in reality, it belongs in one of the other six categories. A false positive case occurs when the classification model classifies a skin lesion image as having melanoma when, in reality, it belongs to one of the other six disorders. If the classifier includes an image of a skin lesion that is not melanoma, then it is a true negative.

We shall now understand the meaning and methodology of the aforementioned measures

TP = True Positive;

FN = False Negative;

FP = False Positive;

TN = True Negative.

For example, this is viewed as a veritable positive case assuming the model likewise shows that the skin injury picture has melanoma and the skin injury picture is recognized as having melanoma. In the doubtful occasion that melanoma is distinguished in the picture yet the picture is arranged into any of the other six classifications, this is an illustration of dishonestly bad data. At the point when the portrayal model sees an image of skin harm as having melanoma when, truth be told, it could be any of the other six problems, this is known as a phony positive event. Should the classifier propose a non-melanoma skin sore picture as non-melanoma, this is a true negative outcome.

- Accuracy

The little percentage of expectations that our model has correctly predicted is called precision.

It is defined as:

$$Accuracy = \frac{TP + TN}{TP + TN + FP + FN}$$

- Precision

The accuracy measure provides an answer to the related question: How accurate were the positive IDs?

It is defined as:

$$Precision = \frac{TP}{TP + FP}$$

- Sensitivity/Recall

The Genuine Positive Rate (TPR) or Review is an alternative term for awareness. It answers the following related query: What percentage of the actual upsides were accurately identified?

It is defined as:

$$Sensitivity = \frac{TP}{TP + FN}$$

- F1 Score

The Genuine Positive Rate (TPR) or Review is another term for awareness. The following question is addressed: To what degree the true benefits were appropriately identified.

It is defined as:

$$F_1 = 2 * \frac{Precision * recall}{precision + recall}$$

- Support

The amount of genuine class events in the pre-established dataset is known as support.

Hyperparameters. Table 6 lists the hyperparameters that were used to configure the CNN models.

Table 6. Hyperparameters That the CNN Models Are Trained Using

Optimizer	Adam optimizer
Learning	0.0002

Epochs	35
Loss function	Categorical cross-entropy
Batch size	65
Dropout	0.5

5.2. Model Performance

- ResNet50

The course of action execution of the ResNet50 model is shrouded in this part. Since this model requires the commitment to be in that configuration, the data pictures have been resized to 229 × 229. Table 7 displays this model's disarray grid. The model's categorization report is shown in Table 8.

Table 7. Matrix of confusion for ResNet50

		TRUE CLASS						
		AKIEC	BCC	BKL	DF	MEL	NV	VASC
PREDICTED CLASS	AKIEC	116	15	78	8	12	11	1
	BCC	32	575	73	5	32	52	3
	BKL	12	18	599	2	30	35	1
	DF	2	6	7	55	7	4	1
	MEL	5	14	105	2	829	172	1
	NV	4	16	118	9	136	3680	3
	VASC	1	2	1	2	1	3	73

Table 8: Report on ResNet50 categorization

	PRECISIO N	RECALL	FI SCORE	SUPPORT
Actinic keratosis	70	49	56	237
Basal cell carcinoma	91	76	82	769
Benign keratosis	62	85	73	700
Dermatofibroma	72	71	72	78
Melanoma	80	73	76	1123
Melanocytic nevus	95	92	92	4000
Vascular lesion	96	90	92	80

Table 9 displays the average metrics the model was able to accomplish.

Table 9: Average metrics for ResNet50

ACCURACY	86
PRECISION	87
RECALL	84
F1 SCORE	86
SUPPORT	7000

- MobileNet

The grouping execution of the MobileNet model is covered in this section. Because this model requires the contribution to be in that configuration, the info photos were shrunk to 229 × 229. Table 10 displays this model's disarray grid.

Table 10: Matrix of Mobile Net Confusing

		True class						
		AKIEC	BCC	BKL	DF	MEL	NV	VASC
Predicted Class	AKIEC	120	21	66	2	21	14	1
	BCC	23	595	58	8	34	58	2
	BKL	12	21	583	1	30	49	1
	DF	2	7	11	43	6	15	1
	MEL	6	19	86	1	783	231	1
	NV	5	27	127	3	54	3800	7
	VASC	1	2	3	2	3	8	67

The model's categorization report is displayed in Table 11.

Table 11: MobileNet classification report

	PRECISION	RECAL L	F1 SCORE	SUPPORT
Actinic keratosis	74	51	60	237
Basal cell carcinoma	88	78	82	769
Benign keratosis	64	86	73	700
Dermatofibroma	80	56	72	78
Melanoma	86	71	76	1123
Melanocytic nevus	92	96	92	4000
Vascular lesion	91	85	92	80

Table 12 displays the average metrics the model was able to accomplish.

Table 12: MobileNet average metrics

ACCURACY	86
PRECISION	87
RECALL	84
F1 SCORE	86
SUPPORT	7000

- VGG16

The VGG16 model's classification performance is shown in this section. The input photographs were reduced in size to 229 × 229 since it was the format needed for this model.

With regard to the model, the confusion matrix is presented in Table 13.

Table 13: Confusion matrix VGG16

PREDICTED CLASS		TRUE CLASS						
		AKIEC	BCC	BKL	DF	MEL	NV	VASC
PREDICTED CLASS	AKIEC	106	45	49	5	20	19	1
	BCC	8	657	32	2	25	48	4
	BKL	10	16	546	3	31	90	1
	DF	2	7	6	46	3	15	4
	MEL	5	23	50	1	825	224	1

	NV	4	24	53	2	94	3800	2
	VASC	1	4	1	2	1	3	72

The model's layout report is shown in Table 14.

Table 14: Report on the categorization of VGG16

	PRECISION	RECALL	F1 SCORE	SUPPORT
Actinic keratosis	82	45	58	239
Basal cell carcinoma	86	86	86	769
Benign keratosis	76	80	78	700
Dermatofibroma	81	59	69	78
Melanoma	84	74	79	1123
Melanocytic nevus	92	97	94	4000
Vascular lesion	92	91	91	80

Table 15 displays the average metrics the model was able to accomplish.

Table 15: VGG16 average metrics

ACCURACY	88
PRECISION	88
RECALL	88
F1 SCORE	88
SUPPORT	6945

- Inception V3

The characterization execution of the Origin V3 model is covered in this section. Because this model requires the contribution to be in that organisation, the info pictures were shrunk to 300 × 300. Table 16 displays this model's disarray network.

Table 16: Confusion matrix for Inception V3

PREDICTED CLASS		TRUE CLASS						
		AKIEC	BCC	BKL	DF	MEL	NV	VASC
PREDICTED CLASS	AKIEC	152	28	36	1	19	8	1
	BCC	16	668	26	6	24	33	2
	BKL	13	19	594	1	35	34	1
	DF	2	4	7	55	3	9	2
	MEL	8	12	40	2	955	111	1
	NV	3	19	58	4	126	3800	2
	VASC	1	1	1	2	1	5	75

The model's grouping report is shown in Table 17.

Table 17: Report on Inception V3 Classification

	PRECISION	RECALL	F1 SCORE	SUPPORT
Actinic keratosis	81	64	72	239
Basal cell carcinoma	90	88	89	769
Benign keratosis	80	87	83	700
Dermatofibroma	80	71	78	78
Melanoma	84	86	85	1123
Melanocytic nevus	96	96	96	4000
Vascular lesion	97	95	96	80

Table 18 displays the average metrics the model was able to accomplish.

Table 18: Average metrics for Inception V3

ACCURACY	91
PRECISION	91
RECALL	91
F1 SCORE	91
SUPPORT	6945

- InceptionResnet V2

This section discusses the InceptionResnet model's order of execution. The information pictures were downsized to 300 x 300 because such organisation is required for this model to work.

Table 19 displays this model's disarray network.

Table 19: Confusion matrix for the initial Resnet

PREDICTED CLASS		TRUE CLASS						
		AKIE C	BCC	BKL	DF	MEL	NV	VASC
AKIE C	AKIE C	143	43	36	1	12	8	1
	BCC	2	718	17	3	15	19	1
	BKL	4	24	613	2	19	33	2
	DF	2	5	6	63	2	5	1
	MEL	6	20	37	1	944	120	1
	NV	1	37	53	5	99	3800	1
	VASC	1	2	1	2	2	3	75

The model's categorization report is shown in Table 20.

Table 20: Report on the initial Resnet categorization

	PRECISION	RECALL	F1 SCORE	SUPPORT
Actinic keratosis	94	61	74	239
Basal cell carcinoma	86	94	90	769
Benign keratosis	82	90	86	700
Dermatofibroma	88	82	85	78
Melanoma	88	85	85	1123
Melanocytic nevus	96	96	96	4000
Vascular lesion	98	95	96	80

Table 21 shows the average metrics the model was able to attain

Table 21. InceptionResnet average metrics

ACCURACY	92
PRECISION	92
RECALL	92
F1 SCORE	92
SUPPORT	6945

5.3. Comparison & Discussion

The midpoints of the last CNNs' seven-illness order for every one of the accompanying measurements are shown in Table 22: exactness, accuracy, review, F1 score, and backing.

Table 22: The mean stats attained by every final CNN

Architecture	Support	Precision (%)	Recall (%)	F1-score (%)	Accuracy(%)
RESNET50	7000	87	86	86	86
MOBILENET	7000	87	86	86	86
VGG16	7000	88	88	88	88
INCEPTION V3	7000	91	91	91	91
INCEPTIONRESNET	7000	92	92	92	92

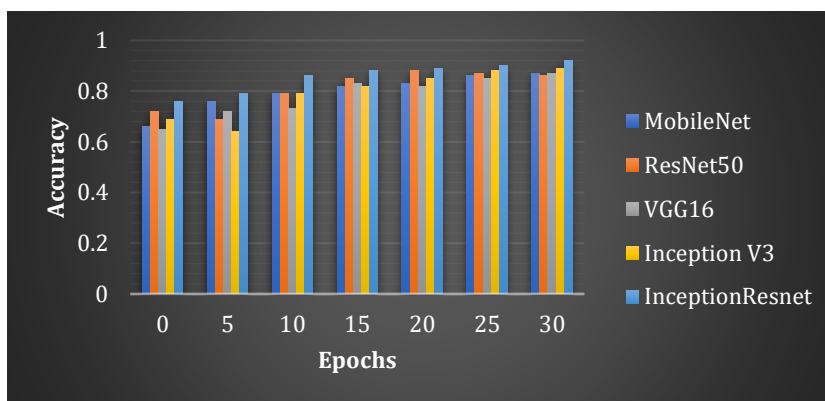


Figure 13: CNN accuracy curves

Figure 13 shows the learning bends for every one of the CNN models. Table 22 and Fig. 14 plainly show that the Commencement V3 and InceptionResnet CNN models have yielded the best outcomes, with 94 and 95% precision in characterization. This model is sufficiently strong to perceive every one of the seven various types of sores in pictures.

6. Conclusion And Future Works

Deep learning techniques for diagnosing and treating skin cancer represent a radical shift in the field of dermatological diagnostics. This writing audit has looked into a few studies that demonstrate the growing field of artificial intelligence—specifically, deep learning—in addressing the challenges associated with the identification of skin cancer. Combining state-of-the-art computational techniques with clinical imaging has ushered in a new era that promises more accurate, skillful, and timely discoveries, ultimately leading to results that are easier to grasp. The capacity of deep learning to autonomously extract complex examples and elements from large datasets is one of its most important features in the field of skin cancer location. This feature's research examined the various applications of deep learning architectures, ranging from half breed models and groups to convolutional neural networks (CNNs). These patterns have an amazing ability to discern distinctions in skin lesions, contributing to increased reactivity and clarity in distinguishing between safe and hazardous situations.

Deep learning approaches can be combined in ways that go beyond a single tactic. Researchers are looking at mixed models, which combine the best features of several computational techniques. These models show a creative fusion of traditional machine learning computations with deep learning architectures. By combining the best features of several approaches, this hybridization aims to overcome the limitations inherent in different ideologies. Furthermore, the literature reviewed emphasises how multidisciplinary these projects are. Coordination between PC researchers and clinical specialists has led to the development of models that are both clinically relevant and demonstrate specialised competence. The validation of deep learning models using many datasets and comprehensive evaluation metrics increases their plausibility and brings us closer to the prospect of validated clinical uses.

Still, there are obstacles to overcome, such as the interpretability of deep learning models and the need for massively diverse datasets for extensive preparation. As these technologies progress, moral considerations, security issues, and organisational frameworks also need careful thought. To guarantee the moral and reliable application of deep learning methods in therapeutic contexts, these issues must be resolved. The majority of the surveyed writing accentuates the entrancing prospects of involving deep learning techniques for skin cancer detection and examination. The progressions in dermatological diagnostics will most likely be basic later on, changing the exactness, adequacy, and openness of skin cancer screening. The pathway to unleashing the full potential of deep learning in the context of understanding consideration and outcomes in the domain of skin cancer conclusion lies in the cooperative energy between clinical mastery and computational development.

In outline, the undertaking's goal was to make a convolutional neural network model that could distinguish and evaluate skin cancer in sores found in photographs.

It likewise explored the data expansion procedure as a preprocessing move toward work on the goodness of the CNN model's characterisation. With a 94% ordinary accuracy, the best model — InceptionResnet specifically — accomplished.

References

- [1] Baratloo, M. Hosseini, A. Negida, G. El Ashal, Part 1: Simple Definition and Calculation of Accuracy, Sensitivity and Specificity. (Emergency, Tehran, Iran, 2015).
- [2] A. Esteva et al., Dermatologist-level classification of skin cancer with deep neural networks. *Nature* (2017)
- [3] A.G. Howard et al., MobileNets. *arXivPrepr. arXiv1704.04861* (2017)
- [4] Abunadi, I., & Senan, E. M. (2021). Deep learning and machine learning techniques of diagnosis dermoscopy images for early detection of skin diseases. *Electronics*, 10(24), 3158.
- [5] Mazhar, T., Haq, I., Ditta, A., Mohsan, S. A. H., Rehman, F., Zafar, I., ... & Goh, L. P. W. (2023, February). The role of machine learning and deep learning approaches for the detection of skin cancer. In *Healthcare* (Vol. 11, No. 3, p. 415). MDPI.
- [6] Gouda, W., Sama, N. U., Al-Waakid, G., Humayun, M., & Jhanjhi, N. Z. (2022, June). Detection of skin cancer based on skin lesion images using deep learning. In *Healthcare* (Vol. 10, No. 7, p. 1183). MDPI.
- [7] Hossin, M. A., Rupom, F. F., Mahi, H. R., Sarker, A., Ahsan, F., & Warech, S. (2020, October). Melanoma skin cancer detection using deep learning and advanced regularizer. In *2020 International Conference on Advanced Computer Science and Information Systems (ICACSIS)* (pp. 89-94). IEEE.
- [8] Adegun, A., & Viriri, S. (2021). Deep learning techniques for skin lesion analysis and melanoma cancer detection: a survey of state-of-the-art. *Artificial Intelligence Review*, 54, 811-841.
- [9] Bassel, A., Abdulkareem, A. B., Alyasseri, Z. A. A., Sani, N. S., & Mohammed, H. J. (2022). Automatic malignant and benign skin cancer classification using a hybrid deep learning approach. *Diagnostics*, 12(10), 2472.
- [10] Tembhrune, J. V., Hebbar, N., Patil, H. Y., & Diwan, T. (2023). Skin cancer detection using ensemble of machine learning and deep learning techniques. *Multimedia Tools and Applications*, 1-24.
- [11] Adla, D., Reddy, G. V. R., Nayak, P., & Karuna, G. (2022). Deep learning-based computer aided diagnosis model for skin cancer detection and classification. *Distributed and Parallel Databases*, 40(4), 717-736.
- [12] Nancy, V. A. O., Prabhavathy, P., Arya, M. S., & Ahamed, B. S. (2023). Comparative study and analysis on skin cancer detection using machine learning and deep learning algorithms. *Multimedia Tools and Applications*, 1-45.
- [13] Inthiyaz, S., Altahan, B. R., Ahammad, S. H., Rajesh, V., Kalangi, R. R., Smirani, L. K., ... & Rashed, A. N. Z. (2023). Skin disease detection using deep learning. *Advances in Engineering Software*, 175, 103361.
- [14] Ashraf, R., Kiran, I., Mahmood, T., Butt, A. U. R., Razaq, N., & Farooq, Z. (2020, November). An efficient technique for skin cancer classification using deep learning. In *2020 IEEE 23rd International Multitopic Conference (INMIC)* (pp. 1-5). IEEE.
- [15] Adegun, A. A., & Viriri, S. (2019). Deep learning-based system for automatic melanoma detection. *IEEE Access*, 8, 7160-7172.
- [16] Alfi, I. A., Rahman, M. M., Shorfuzzaman, M., & Nazir, A. (2022). A non-invasive interpretable diagnosis of melanoma skin cancer using deep learning and ensemble stacking of machine learning models. *Diagnostics*, 12(3), 726.
- [17] Ali, M. S., Miah, M. S., Haque, J., Rahman, M. M., & Islam, M. K. (2021). An enhanced technique of skin cancer classification using deep convolutional neural network with transfer learning models. *Machine Learning with Applications*, 5, 100036.
- [18] American Cancer Society, "Cancer Facts and Figures 2019." [Online]. Available: <https://www.cancer.org/content/dam/cancer-org/research/cancer-facts-and-statistics/annual-cancer-facts-and-figures/2019/cancer-facts-and-figures-2019.pdf>.
- [19] C. Szegedy, S. Ioffe, V. Vanhoucke, A.A. Alemi, Inception-v4, inception-ResNet and the impact of residual connections on learning, in *31st AAAI Conference on Artificial Intelligence, AAAI 2017* (2017)
- [20] Krishna, T., Praveen, S. P., Ahmed, S., & Srinivasu, P. N. (2023). Software-driven secure framework for mobile healthcare applications in IoMT. *Intelligent Decision Technologies*, 17(2), 377-393.
- [21] Codella, N., Rotemberg, V., Tschandl, P., Celebi, M. E., Dusza, S., Gutman, D., ... & Halpern, A. (2019). Skin lesion analysis toward melanoma detection 2018: A challenge hosted by the international skin imaging collaboration (isic). *arXiv preprint arXiv:1902.03368*.
- [22] Praveen, S. P., Thati, B., Anuradha, C., Sindhura, S., & Altaee, M. (2023). A novel approach for enhance fusion based healthcare system in cloud computing. *Full Length Article*, 9(1), 84-4.
- [23] Das, K., Cockerell, C. J., Patil, A., Pietkiewicz, P., Giulini, M., Grabbe, S., & Goldust, M. (2021). Machine learning and its application in skin cancer. *International Journal of Environmental Research and Public Health*, 18(24), 13409.

- [24] Praveen, S. P., Jyothi, V. E., Anuradha, C., VenuGopal, K., Shariff, V., & Sindhura, S. (2022). Chronic kidney disease prediction using ML-based Neuro-Fuzzy model. *International Journal of Image and Graphics*, 2340013.
- [25] H., Mina, M., Abbas, M., Kadhim, Alaa, M., El-Sayed. Enhancement CNN based on LSTM for vital sign classification. *Journal of Fusion: Practice and Applications*, vol. 13, no. 2, 2023, pp. 22-33. DOI: <https://doi.org/10.54216/FPA.130202>
- [26] International Skin Imaging Collaboration, "ISIC 2018: Skin Lesion Analysis Towards Melanoma Detection," 2018. [Online]. Available: <https://challenge2018.isic-archive.com/> Accessed: 29-Oct-2019
- [27] Prasad, Maruthi, R., Santhosh. Randomized Vector Network Model for Thyroid Prediction Using Relief And Lasso Feature Selection Approaches. *Journal of Fusion: Practice and Applications*, vol. 12, no. 2, 2023, pp. 132-144. DOI: <https://doi.org/10.54216/FPA.120211>
- [28] Venkatesh, K. Pasupathy, S. P., S. (2023). A Learning Model for Acute Myeloid Leukemia Prediction Using Dense Polynomial Dimensionality-Based Predictor. *Journal of Fusion: Practice and Applications*, 12(2), 145-158. DOI: <https://doi.org/10.54216/FPA.120212>
- [29] Madhuri, A., Jyothi, V. E., Praveen, S. P., Altaee, M., & Abdullah, I. N. (2023). Granulation-Based Data Fusion Approach for a Critical Thinking Worldview Information Processing. *Journal of Intelligent Systems and Internet of Things*, 9(1), 49-68.
- [30] Li, Y., & Shen, L. (2018). Skin lesion analysis towards melanoma detection using deep learning network. *Sensors*, 18(2), 556.
- [31] Maurya, S., Tiwari, S., Mothukuri, M. C., Tangeda, C. M., Nandigam, R. N. S., & Addagiri, D. C. (2023). A review on recent developments in cancer detection using Machine Learning and Deep Learning models. *Biomedical Signal Processing and Control*, 80, 104398.
- [32] Praveen, S. P., Murali Krishna, T. B., Anuradha, C. H., Mandalapu, S. R., Sarala, P., & Sindhura, S. (2022). A robust framework for handling health care information based on machine learning and big data engineering techniques. *International Journal of Healthcare Management*, 1-18.
- [33] P. Tschandl, C. Rosendahl, H. Kittler, Data descriptor: the HAM10000 dataset, a large collection of multi-sourcedermatoscopic images of common pigmented skin lesions. *Sci. Data* (2018)
- [34] Pacheco, A. G., & Krohling, R. A. (2019). Recent advances in deep learning applied to skin cancer detection. arXiv preprint arXiv:1912.03280.
- [35] Rahi, M. M. I., Khan, F. T., Mahtab, M. T., Ullah, A. A., Alam, M. G. R., & Alam, M. A. (2019, December). Detection of skin cancer using deep neural networks. In 2019 IEEE Asia-Pacific Conference on Computer Science and Data Engineering (CSDE) (pp. 1-7). IEEE.
- [36] Rezk, E., Eltorki, M., & El-Dakhakhni, W. (2022). Improving skin color diversity in cancer detection: deep learning approach. *JMIR Dermatology*, 5(3), e39143.
- [37] Srinivasu, P. N., Sirisha, U., Sandeep, K., Praveen, S. P., Maguluri, L. P., & Bikku, T. (2024). An Interpretable Approach with Explainable AI for Heart Stroke Prediction. *Diagnostics*, 14(2), 128.
- [38] Shah, V., Autee, P., & Sonawane, P. (2020, December). Detection of melanoma from skin lesion images using deep learning techniques. In 2020 International Conference on Data Science and Engineering (ICDSE) (pp. 1-8). IEEE.
- [39] Singh, S. K., Abolghasemi, V., & Anisi, M. H. (2023). Fuzzy logic with deep learning for detection of skin cancer. *Applied Sciences*, 13(15), 8927.
- [40] Sri Geetha, M., Selvarani, A. G., Kumar, R., Degadwala, S., & Veluri, R. K. (2021). Automatic Detection and Classification Of Melanoma Skin Cancer through Deep Learning Techniques. *NVEO-NATURAL VOLATILES & ESSENTIAL OILS Journal| NVEO*, 7584-7594.
- [41] Thapar, P., Rakhra, M., Cazzato, G., & Hossain, M. S. (2022). A novel hybrid deep learning approach for skin lesion segmentation and classification. *Journal of Healthcare Engineering*, 2022.
- [42] Tlaisun, L., Hussain, J., Hnamte, V., Chhakchhuak, L., & Hmar, L. (2023). Efficient Deep Learning Approach for Modern Skin Cancer Detection. *Indian Journal of Science and Technology*, 16, 110-120.
- [43] Viknesh, C. K., Kumar, P. N., Seetharaman, R., & Anitha, D. (2023). Detection and Classification of Melanoma Skin Cancer Using Image Processing Technique. *Diagnostics*, 13(21), 3313.
- [44] World Cancer Research Fund - Skin Cancer Statistics, 2018. [Online]. Available: <https://www.wcrf.org/dietandcancer/cancer-trends/skin-cancer-statistics>. Accessed: 28-Oct-2019
- [45] Zafar, M., Sharif, M. I., Sharif, M. I., Kadry, S., Bukhari, S. A. C., & Rauf, H. T. (2023). Skin lesion analysis and cancer detection based on machine/deep learning techniques: A comprehensive survey. *Life*, 13(1), 146.